PRELIMINARY

SNO -STR-91-19

DRAFT

Extraction of CC NC and ES Signals - II
Acrylic Radioactivity
Three Parameter Maximum Likelihood Analysis

W. Frati and E. Beier
Univ of Pennsylvania

Feb 13 1991

1 Introduction

In SNO-STR-88-87 a study was presented of systematic effects in extracting the CC, NC and ES scattering signals under the three running conditions of light water, heavy water, and salt + heavy water. In that analysis only the inner half of the volume contained within the then cylindrical acrylic vessel was used in order to beg the question of the radial dependence of the externally induced background. This enabled us to limit the number of parameters in the Maximum Likelihood Analysis (MLA) to two; a) the energy and b) the angle of the event relative to the sun (θ_{sun}). In this report we expand the analysis to the full volume of the detector viewed by the light cones, which includes the one meter of light water outside the acrylic, and now use the radial distribution of the events as a third parameter in the MLA. Specifically we address the question; "What is the effect of having an acrylic radioactivity that is ten times the white book value". Further, we now have the individual events generated by Queens, whereas previously only the Energy-cos(θ_{sun}) two-dimensional histogram generated by UCI was available.

2 Theoretical Functions

2.1 Overview

While the NC background generated by the acrylic is now included in the analysis, the PMT $\beta\gamma$ and external γ backgrounds are omitted, which limits the analysis to energies

greater than 6 MeV. Results are also presented with an energy starting at 5 MeV, but it should be kept in mind that the omitted backgrounds will play a role at 5 MeV, especially for the H_2O signal, and eventually will have to be incorporated. The NC generated by radioactivity in the H_2O is small relative to that generated by the acrylic and is also ignored in this analysis. Thus five signals are used in the analyses presented here.

- 1 Charged Current
- 2 Neutral Current (Internal + Solar)
- 3 Elastic Scattering in the D_2O
- 4 Elastic Scattering in the H_2O
- 5 Neutral Current induced by acrylic radioactivity.

Table I summarizes the events provided by Queens, from which two things are obtained: 1) One year of 'data' from a sampling of these events 2) The functional form of the five reactions as a function of the three variables, NPMT = N, $\cos(\theta_{sun})$ = u, and radius for which the natural variable R^3 is used. It is important to note that R^3 and $\cos(\theta_{sun})$ are the reconstructed vertex and direction as opposed to the generated values. The energy of the event depends primarily on the number of PMT's in the event, and for this analysis a linear relationship is assumed, where the scale is approximately 10 PMT's/MeV.

The signal $G(N, u, R^3)$ is the weighted sum of the five reactions represented by the functions $F_k(N, u, R^3)$;

$$G(N, u, R^3) = \sum_{k=1}^{5} w_k F_k(N, u, R^3)$$

where the w_K are the amplitudes to be extracted by the analysis. It would be extremely fortuitous to find analytic expressions for $F_k(N, u, R^3)$ that includes all the correlations and this is not attempted. A 3D histogram of the events could be easily generated, but this is precluded by the large number of Monte Carlo events that would have to be generated to result in a statistically significant number of events in each

bin. Consider for example 100 years of CC events, which amounts to $\approx$ 500k events. Dividing NPMT, $\cos(\theta_{sun})$ and R^3 into 50 intervals each means there will only be ≈ 4 events/bin on average, and only 0.4 events/bin for the ES signal. Thus factorization of the $F_k(N, u, R^3)$ is resorted to. The factorization and parametrization of these functions are now discussed in turn for each of the five reactions and for the D_2O and D_2O plus Chlorine fills.

2.2 Charged Current and Neutral Current(Chlorine in)

2.2.1 Radial Distributions

Fig 1a shows the R^3 distributions for events with NPMT$\geq$ 60 for the complete NC and CC data sets listed in Table I. Both reactions are well represented by the functional form:

$$F(z) = \frac{1 - \alpha z}{1 + \beta e^{\gamma z}}$$

The best fits are the smooth curves overlaying the histogrammed data sets in Fig 1. Appendix I lists the parametric form and the parameters resulting from the best fit.

2.2.2 NPMT Distributions

These distributions are shown in Fig 1b, along with the best fit functional forms, which are simple Gaussians. The overall shapes are fitted well by the Gaussians, but a structure in noted in the data sets which is not yet understood. A logarithmic plot is shown in Fig 1c.

2.2.3 $\cos(\theta_{sun})$ Distributions

The neutral current is of course isotropic, and the charged current is linear in $\cos(\theta_{sun})$, with a theoretical coefficient $\alpha = -1/3$. Fig 1d displays the $\cos(\theta_{sun})$ distributions from the event reconstruction, with a straight line fit yielding $\alpha = -0.297 \pm 0.005$. There is a correlation between α and NPMT, which is shown in Fig 1e, where the α's derived from the generated and reconstructed directions are shown as a function of NPMT. The α derived from the generated direction is flat at 1/3, while those obtained from the

reconstruction show α increasing with NPMT and approaching the theoretical value of 1/3 as NPMT increases.

2.3 Elastic Scattering in D_2O and H_2O

2.3.1 Radial Distributions

The R^3 distribution for D_2O events is represented by the same function used in the charged current distribution. The H_2O events are represented by the so called Extreme Value Distribution;

$$F(z) = \exp[v - e^v]$$
$$v = \frac{\alpha - z}{\beta}$$

The event distributions along with the functional forms are shown in Fig 2a.

2.3.2 NPMT Distributions

Gaussian functions represent these distributions well as shown in Fig 2b. The D_2O and H_2O have somewhat different shapes, with the H_2O events falling towards slightly smaller numbers of PMT's.

2.3.3 $\cos(\theta_{sun})$ Distributions

The $\cos(\theta_{sun})$ distributions integrated over NPMT $\geq$ 60 are fitted to the sum of two exponentials. These distributions along with the best fits are shown in Fig 2c. As in the case of the charged current events, these distributions have correlations with NPMT. Fig 2d shows four $\cos(\theta_{sun})$ distributions (D_2O events) for NPMT intervals of (20-29), (30-39), (40-49) and (50-59) superimposed with an exponential fit. Fig 2e shows similar plots for NPMT intervals of (100-109), (110-119), (120-129) and (130-139). These are each well fit by $e^{\alpha u}$ where Fig 2f shows α increasing linearly with NPMT. Fig 2g shows a similar plot for the H_2O events, which also shows a rise of α with NPMT, but with a somewhat shallower slope and a levelling off at about 140 PMT's.

2.4 Neutral Current from Acrylic (D_2O + Cl)

Both the R^3 and NPMT distributions are fit to the sum of two Gaussians and are shown in Fig 3a and Fig 3b resp. The χ^2 are $\approx$ 2 and 4 per degree of freedom for the R^3 and NPMT distributions resp. As in the case of the CC NPMT distributions some structure is noted.

2.5 Neutral Current (D_2O Only)

Both the R^3 and NPMT distributions are fit to the sum of two Gaussians and are shown in Fig 4a and Fig 4b resp. The χ^2 are $\approx$ 1 and 6 per degree of freedom for the R^3 and NPMT distributions resp. The sharp peak sitting on top of the NPMT distribution makes a better fit difficult to achieve.

2.6 Neutral Current from Acrylic (D_2O Only)

The R^3 distribution is fit to the sum of two Gaussians. There are only 816 events with NPMT $\geq$ 60, and the χ^2/DoF of freedom is $\approx$ 1. The NPMT distribution is fit to a single Gaussian, with a χ^2/DoF again approximately one. These distributions are shown in Fig 5a and Fig 5b.

3 Generalized Maximum Likelihood Method

The weightings w_k for each of the five components in the signal

$$G(N, u, \mathrm{R}^3) = \sum_{k=1}^{5} w_k F_k(N, u, \mathrm{R}^3)$$

are determined by maximizing the Likelihood Function

$$L(w_k) = \sum_{n=1}^{Nev} lnG - \int_{N_{min}}^{N_{max}} \int_{u_{min}}^{u_{max}} \int_{\mathrm{R}^3{}_{min}}^{\mathrm{R}^3{}_{max}} G(N, u, \mathrm{R}^3)\, dN\, du\, d\mathrm{R}^3$$

Note that the sum is over the individual events. Normalizing $F_k(N, u, \mathrm{R}^3)$ such that

$$\int_{N_{min}}^{N_{max}} \int_{u_{min}}^{u_{max}} \int_{\mathrm{R}^3{}_{min}}^{\mathrm{R}^3{}_{max}} F_k(N, u, \mathrm{R}^3)\, dN\, du\, d\mathrm{R}^3 = 1$$

the Maximum Likelihood Function reduces to

$$L(w_k) = \sum_{n=1}^{Nev} lnG - \sum_{k=1}^{5} w_k$$

where w_k are now the number of events in the component signals. The CERN program MINUIT is used to maximize the Likelihood Function.

4 Results

4.1 'Standard' D_2O +Cl

The 'standard' conditions are taken to mean:

- White Book values for the acrylic radioactivity.
- NPMT $\geq$ 60 (6 MeV).
- R $\leq$ 7 meters.
- Functional forms as defined in the previous sections.
- One year of data.
- Sampling every third event from the data set in Table I.

The numbers of events generated and the numbers extracted by the MLA are summarized in Table II, (reproduced below) where the numbers in parenthesis are the statistical errors.

MLA RESULTS of 'STANDARD' EVENTS

Reaction	Generated	Extracted	Ratio (E/G)
CC	2241	2171(111)	0.94(0.05)
NC	2315	2367(117)	1.02(0.05)
ES(D_2O)	219	227(30)	1.04(0.14)
ES(H_2O)	110	117(13)	1.06(0.12)
Acrylic	234	239(55)	1.02(0.24)
SUM	5119	5121	

The extracted numbers merely reflect what was put in and serve as a check. This was further checked by taking different event samples, and is summarized in Table III. The statistical errors are larger than the square root of the number of events, implying correlations exist. Fig 6a shows the equal probability contours for the NC-CC pairing where it is seen that the correlation is very strong, in contrast to the CC-ESH_2O pairing shown in Fig 6b which has virtually no correlation. The strong correlation between the NC and CC might be expected since this is the pairing of signals that has the greatest similarity in the three variables. Table IV shows the correlation matrix for all pairings of signals. The statistical accuracy in determining the CC and NC signals is 5%, while that of the ES events in the D_2O and H_2O are in the 10-15% range. Systematic effects are discussed later.

Fig 7a shows the overlay of the NPMT distribution with the MLA results and Fig 7b shows the contribution of the various components. Figs 7c and 7d are similar plots for the R^3 distribution and Figs 7e and 7f for $\cos(\theta_{sun})$.

4.2 X10 Acrylic Radioactivity (D_2O +Cl)

The number of NC events from acrylic radioactivity that is put into the 'data' set is increased ten-fold and the analysis repeated. The results are listed in Table V and reproduced below. The exercise is repeated for different data sets with the results shown in Table VI.

MLA RESULTS of x10 ACRYLIC RADIOACTIVITY

Reaction	Generated	Extracted	Ratio (E/G)
CC	2241	1979(115)	0.88(0.05)
NC	2315	2549(123)	1.10(0.05)
ES(D_2O)	219	216(32)	0.99(0.15)
ES(H_2O)	110	135(16)	1.23(0.15)
Acrylic	2344	2347(78)	1.00(0.03)
SUM	7229	7226	

The following are noted.

- The statistical accuracy in extracting the various component signals is NOT significantly affected by a ten-fold increase acrylic radioactivity.
- Systematic effects at the 10% level occur, with the extracted NC, CC and ESH_2O signals being off by two standard deviations. The feature that the NC and ESH_2O are systematically high and the CC is systematically low appears to hold even when other data sets are used, as shown in Table VI.
- The NC, CC correlation manifests itself more prominently here than in the 'standard' event sample in that the CC produces a low result, while the NC produces a high result.
- It is not understood why the ESH_2O is systematically high, since its correlations with the other signals are weak as shown in Table IV.

Figs 8a-8f display the NPMT, R^3 and $\cos(\theta_{sun})$ distributions along with the fits from the MLA.

4.3 D_2O Only

The 'standard' and x10 acrylic radioactivity scenarios are run with only D_2O (no Chlorine) inside the acrylic. Tables VII and VIII summarizes the results. Figs 9a-9f display

the results for the X10 acrylic radioactivity run. Fig's 9a,9c and 9d show two smooth curves overlaying the histogrammed data. One is the generating function and the other the best fit.

The following are noted:

- Compared to the Chlorine fill, the statistical accuracy on the charged current improves a factor of two (5.0% to 2.5%). The NC gets worse, going from 5% to 28%. This is primarily due to the 6 MeV cut imposed on the data.
- Compared to the Chlorine fill, the statistical accuracy of the ES signals marginally improves.
- The acrylic signal cannot be determined in the 'standard' data set, and in the X10 scenario can only be determined to 40%.
- No significant change in the statistical accuracy occurs when the acrylic radioactivity is increased ten-fold, nor are any systematic effects introduced.

Table IX summarizes the percentage statistical accuracy of the 'standard' and x10 acrylic radioactivity scenarios for both the D_2O + Cl and D_2O only fills. Also included in this table are the results of the analyses performed with $E \geq 5MeV$, keeping in mind that the $\beta\gamma$ background is not included. Note the better than factor of two improvement in the statistical accuracy of the NC for the D_2O only fill when going from a 6 MeV to a 5 MeV threshold.

5 Systematic Studies

Variations are made in both $F_k(N, u, R^3)$ and the input 'data', to study the sensitivity of the extracted amplitudes to systematic effects. This report studies the following for the D_2O + Chlorine fill, for both the 'standard' and the x10 acrylic radioactivity data sets.

- The central value of the radial distribution of the NC signal from the acrylic radioactivity is moved out by 20 cm.

- The width of the radial distribution of the NC signal from the acrylic radioactivity is increased by 20%
- Increasing the energy of each event by 2%.
- Introducing the NPMT-$\cos(\theta_{sun})$ correlations into the ES and CC $F_k(N, u, R^3)$.
- Increasing the coefficient (α) in $(1 - \alpha\cos(\theta_{sun}))$ for the CC angular distribution by 10%.
- Degrading the ES angular resolution by 20% in $F_k(N, u, R^3)$.
- Wobbling the energy of the input event with a Gaussian spread of 10%. The is over and above the inherent energy resolution of the detector at 10 MeV, which is $\approx$ 13%.

The results are shown in Table X for the white book value of the acrylic radioactivity and Table XI for the x10 acrylic radioactivity runs, and are expressed as the ratio of the extracted amplitudes with the systematic effect included to that without any systematic effect.

The following are noted:

- As might be expected, the effect of changing the acrylic radial distribution gives rise to a bigger systematic effect on the solar neutrino signals ($\approx$ 10% more) for the x10 acrylic case than for the x1 case where the effects are only several percent. Thus if the acrylic radioactivity is ten times higher than what we are aiming for, then the radial distribution of the induced NC will have to be determined with greater accuracy than if the white book values of radioactivity are achieved. The extracted amplitude of the acrylic signal changes significantly for the both the x1 and x10 acrylic runs.
- Increasing the energy of each event by 2% causes a systematic increase of $\approx$ 20% for the CC signal and a corresponding 20% decrease in the NC and acrylic signal for the 'standard' scenario. Increasing in the energy of the events results in more events at higher energies and the MLA compensates for this by increasing the CC signal which is the primary source of the higher energy events. Increasing the

acrylic activity ten-fold results in a systematic shift of almost the same magnitude as for the x1 case.

- Degrading the angular resolution of the ES events by 20% gives rise to systematic effects of up to 30% in the amplitude of the ES signals.
- Inserting the correlation between NPMT and $\cos(\theta_{sun})$ has no effect, and disappointingly does not improve the statistical accuracy of the ES and CC amplitudes.
- Changing the coefficient of the CC angular distribution by 10% has little effect.
- Introducing an additional 10% energy resolution in quadrature to the natural resolution of the detector ($\approx$ 13% at 10 MeV) gives rise to systematic effects of $\approx$ 20% for the NC, CC, and ESD_2O signals for the 'standard' events, and increases to 30% when the acrylic activity is increased ten-fold.

6 CONCLUSIONS

Increasing the acrylic radioactivity ten-fold does not present a major problem, but introduces systematic errors of $\approx$ 10% even with an accurate knowledge of acrylic geometry and energy resolution. Uncertainties in the acrylic geometry and energy resolution further aggravate the systematic uncertainties when the acrylic radioactivity is increased ten-fold. Thus a more accurate determination of the spatial characteristics of the NC events induced by the acrylic radioactivity and a more accurate determination of our energy resolution is required should the acrylic radioactivity be larger than anticipated.

Table I

MONTE CARLO EVENTS

Reaction	Years	Events Generated	Events $N \geq 60$ $R_{rec} \leq 7$	Events $N \geq 50$ $R_{rec} \leq 7$
CC	23.3	100k	52k	67k
NC(Cl)	20.3	100k	47k	71k
NC(D_2O)	78.2	100k	12k	41k
ES(D_2O)	35.8	40k	7.8k	11k
ES(H_2O)	35.8	74k	3.9k	5.7k
Acr(Cl)	100	56k	23k	38k
Acr(D_2O)	100	8k	0.81k	2.9k

Table II

MLA RESULTS of "STANDARD" EVENTS

Reaction	Generated	Extracted	Ratio (E/G)
CC	2241	2171(111)	0.97(0.05)
NC	2315	2367(117)	1.02(0.05)
ES(D_2O)	219	227(30)	1.04(0.14)
ES(H_2O)	110	117(13)	1.06(0.12)
Acrylic	234	239(55)	1.02(0.24)
SUM	5119	5121	

Table III

MLA RESULTS 'STANDARD'

Different Event Sampling

	CC	NC	ESD_2O	ESH_2O	Acrylic
Gen	2241	2315	219	110	234
Samp Rate					
1/3	2171(111)	2367(117)	227(30)	117(13)	239(55)
1/5	2136(113)	2305(119)	236(30)	112(13)	330(55)
1/7	2456(116)	2133(119)	168(29)	117(13)	245(53)
1/9	2197(112)	2286(118)	245(31)	115(13)	275(55)
Avg	2240(58)	2273(59)	219(15)	115(7)	272(28)
Avg/Gen	1.00(.03)	0.98(.03)	1.00(.07)	1.04(.06)	1.16(.12)

Table IV

COVARIANCE MATRIX

	CC	NC	ESD_2O	ESH_2O	Acrylic
CC	x	-0.71	-0.04	0.05	-0.15
NC	-0.71	x	-0.15	-0.01	-0.27
ESD_2O	-0.04	-0.15	x	-0.04	-0.02
ESH_2O	0.05	-0.01	-0.04	x	-0.14
Acrylic	-0.15	-0.27	-0.02	-0.14	x

Table V

MLA RESULTS of x10 ACRYLIC RADIOACTIVITY

Reaction	Generated	Extracted	Ratio (E/G)
CC	2241	1979(115)	0.88(0.05)
NC	2315	2549(123)	1.10(0.05)
ES(D_2O)	219	216(32)	0.99(0.15)
ES(H_2O)	110	135(16)	1.23(0.15)
Acrylic	2344	2347(78)	1.00(0.03)
SUM	7229	7226	

Table VI

MLA RESULTS X10 ACRYLIC

Different Event Sampling

	CC	NC	ESD_2O	ESH_2O	Acrylic
Gen	2241	2315	219	110	2344
Samp Rate					
1/3	1979(115)	2549(123)	216(32)	135(16)	2347(78)
1/5	1983(115)	2475(123)	231(33)	125(16)	2411(77)
1/7	2309(122)	2255(125)	147(31)	135(15)	2379(77)
1/9	2059(117)	2407(123)	228(33)	126(15)	2404(78)
Avg	2082(59)	2421(62)	206(16)	130(7)	2385(39)
Avg/Gen	0.93(.03)	1.05(.03)	0.94(.07)	1.18(.06)	1.02(.02)

Table VII

MLA RESULTS D_2O only - 'Standard'

Reaction	Generated	Extracted	Ratio (E/G)
CC	2241	2217(58)	0.99(0.026)
NC	149	163(42)	1.09(0.28)
ES(D_2O)	219	211(24)	0.96(0.11)
ES(H_2O)	110	113(12)	1.02(0.11)
Acrylic	8	23(30)	2.88(3.75)
SUM	2727	2727	

Table VIII

MLA RESULTS D_2O only - X10 ACRYLIC

Reaction	Generated	Extracted	Ratio (E/G)
CC	2241	2208(59)	0.99(0.026)
NC	149	165(44)	1.10(0.30)
ES(D_2O)	219	214(24)	0.98(0.11)
ES(H_2O)	110	115(12)	1.05(0.11)
Acrylic	82	97(34)	1.18(0.41)
SUM	2801	2799	

Table IX

PERCENTAGE STATISTICAL ACCURACY

Acrylic	CC	NC	ESD_2O	ESH_2O	Acrylic
			$N \geq 60$		
			$D_2O + Cl$		
x1	5.0	5.1	13.7	11.8	23.5
x10	5.1	5.3	14.6	14.5	3.3
			$N \geq 60$		
			D_2O ONLY		
x1	2.6	28.2	11.0	10.9	x
x10	2.7	29.5	11.0	10.9	43.0
			$N \geq 50$		
			$D_2O + Cl$		
x1	4.9	4.3	12.3	9.3	17.5
x10	5.3	4.5	13.2	9.9	2.5
			$N \geq 50$		
			D_2O Only		
x1	2.5	11.1	9.4	8.7	x
x10	2.5	11.1	9.4	9.3	17.7

Table X

SYSTEMATIC VARIATIONS 'STANDARD' D_2O + Cl

Variation	CC	NC	ESD_2O	ESH_2O	Acrylic
Acrylic radius	1.02	1.03	1.01	1.00	0.55
Acrylic σ_R	1.01	1.00	1.00	1.00	0.81
1.02 NPMT	1.19	0.83	1.09	1.03	0.82
$\cos(\theta_{\text{sun}})$ -NPMT Corr	1.00	0.99	1.02	0.97	1.02
$1.1 \times \alpha\cos(\theta_{\text{sun}})$ -CC	0.99	1.00	1.04	1.00	1.00
1.2× ES ang res	0.99	0.99	1.30	1.10	0.87
$1.1\sigma_{NPMT}$	1.19	0.80	1.19	1.02	1.05
×10 Acrylic	0.91	1.08	0.95	1.15	9.82

Table XI

SYSTEMATIC VARIATIONS X10 ACRYLIC D_2O + Cl

Variation	CC	NC	ESD_2O	ESH_2O	Acrylic
Acrylic radius	1.08	1.13	1.06	0.87	0.79
Acrylic σ_R	1.05	0.94	1.04	0.87	1.03
1.02 NPMT	1.26	0.81	1.11	1.07	0.97
$\cos(\theta_{\text{sun}})$ -NPMT Corr	1.00	1.00	1.01	0.93	1.01
$1.1 \times \alpha\cos(\theta_{\text{sun}})$ -CC	0.99	1.00	1.05	1.00	1.00
1.2× ES ang res	0.99	0.99	1.28	1.24	0.98
$1.1\sigma_{NPMT}$	1.33	0.72	1.27	1.07	0.98

APPENDIX I

Functional Forms and Their Parameters

$$E(\alpha, z) = \exp(\alpha z)$$

$$G(\alpha, \beta, z) = \exp[(z - \alpha)^2/(2\beta^2)]$$

$$F(\alpha, \beta, \gamma, z) = \frac{1 - \alpha z}{1 + \beta e^{\gamma z}}$$

$$EVF(\alpha, \beta, z) = \exp[v - e^v] : \quad v = \frac{\alpha - z}{\beta}$$

The parameters are listed below with the functional abbreviations defined above.

- Charged Current

  NPMT: G(61.45, 24.42)

  R^3 : F(0.14449e-02, 0.56118e-07, 0.76122e-01)

  $\cos(\theta_{sun})$: 1. - .2968$\cos(\theta_{sun})$

- Neutral Current D_2O + Chlorine

  NPMT: G(59.18, 15.42)

  R^3 : F(0.12743e-02, 0.70052e-02, 0.2666e-01)

  $\cos(\theta_{sun})$: Isotropic

- ES D_2O

  NPMT: G(28.40, 35.60)

  R^3 : F(0.16953e-02, 0.6828e-07, 0.74586e-01)

  $\cos(\theta_{sun})$: 0.814*E(8.1568) + 4.5453*E(3.5974)

- ES H_2O

  NPMT: G(6.146, 42.149)

  R^3 : EVF(277.23, 45.975)

  $\cos(\theta_{sun})$: 1.2145*E(6.9980) + 2.3277*E(1.5331)

- Acrylic D_2O + Chlorine

  NPMT: 750.65 G(49.51, 11.01) + 914.7 G(62.36, 15.30)

  R^3 : 911.96*G(179.63, 48.80) + 44.036*G(292.21, 53.75)

  $\cos(\theta_{sun})$: Isotropic

- NC D_2O Only

  NPMT: 3943.5*G(47.66, 9.73) + 120.18*G(56.84, 11.46)

  R^3 : 691.91*G(-91.48, 132.82) + 30.21*G(270.13, 29.29)

  $\cos(\theta_{sun})$: Isotropic

- Acrylic D_2O Only

  NPMT: G(47.31, 9.92)

  R^3 : 15.73*G(130.56, 86.62) + 8.80*G(266.4, 26.17)

  $\cos(\theta_{sun})$: Isotropic

FIGURE CAPTIONS

- Figure 1. Charged current and neutral current with Chlorine

  (a) R^3 : Generated and functional fit. Solid-CC Dash-NC

  (b) NPMT: Generated and functional fit. Solid-CC Dash-NC

  (c) NPMT: Generated and functional Fit on a log scale

  (d) $\cos(\theta_{sun})$: Reconstructed direction of CC events. NPMT $\geq$ 60 and R $\leq$ 7.

  (e) Coefficient of $\cos(\theta_{sun})$ term for CC events vs NPMT. Solid - generated direction. Dash - reconstructed direction

- Figure 2. Elastic scattering D_2O and H_2O

  (a) R^3 : Generated and functional fit. Dash-D_2O Solid-H_2O

  (b) NPMT: Generated and functional fit. Solid-D_2O Dash-H_2O

  (c) $\cos(\theta_{sun})$: Reconstruced direction Solid-D_2O Dash-H_2O

  (d)$\cos(\theta_{sun})$ in various low NPMT intervals for D_2O

  (e)$\cos(\theta_{sun})$ in various high NPMT intervals for D_2O

  (f)α in $e^{\alpha\cos(\theta_{sun})}$ vs NPMT for D_2O

  (g)α in $e^{\alpha\cos(\theta_{sun})}$ vs NPMT for H_2O

- Figure 3. NC from acrylic radioactivity (D_2O plus Chlorine)

  (a) R^3 : Generated and functional fit.

  (b) NPMT: Generated and functional fit.

- Figure 4. NC (D_2O only)

  (a) R^3 : Generated and runctional Fit.

  (b) NPMT: Generated and functional Fit.

- Figure 5. NC from acrylic radioactivity (D_2O only)

  (a) R^3 : Generated and functional fit.

  (b) NPMT: Generated and functional fit.

- Figure 6. Correlation matrix from MLA
  - (a) NC - CC correlation.
  - (b) CC - ESH_2O correlation.
- Figure 7. Results of MLA for "Standard" (D_2O + Cl)
  - (a) NPMT: Generated and best fit
  - (b) Contribution to NPMT from the five signals
  - (c) R^3 : Generated and best fit
  - (d) Contribution to R^3 from the five signals
  - (e) $\cos(\theta_{sun})$: Generated and best fit
  - (f) Contribution to $\cos(\theta_{sun})$ from the five signals
- Figure 8. Results of MLA for ten-fold increase in acrylic radioactivity.(D_2O + Cl)
  - (a) NPMT: Generated and best fit
  - (b) Contribution to NPMT from the five signals
  - (c) R^3 : Generated and best fit
  - (d) Contribution to R^3 from the five signals
  - (e) $\cos(\theta_{sun})$: Generated and best fit
  - (f) Contribution to $\cos(\theta_{sun})$ from the five signals
- Figure 9. Results of MLA for ten-fold increase in acrylic radioactivity.(D_2O only)
  - (a) NPMT: Generated and best fit
  - (b) Contribution to NPMT from the five signals
  - (c) R^3 : Generated and best fit
  - (d) Contribution to R^3 from the five signals
  - (e) $\cos(\theta_{sun})$: Generated and best fit
  - (f) Contribution to $\cos(\theta_{sun})$ from the five signals

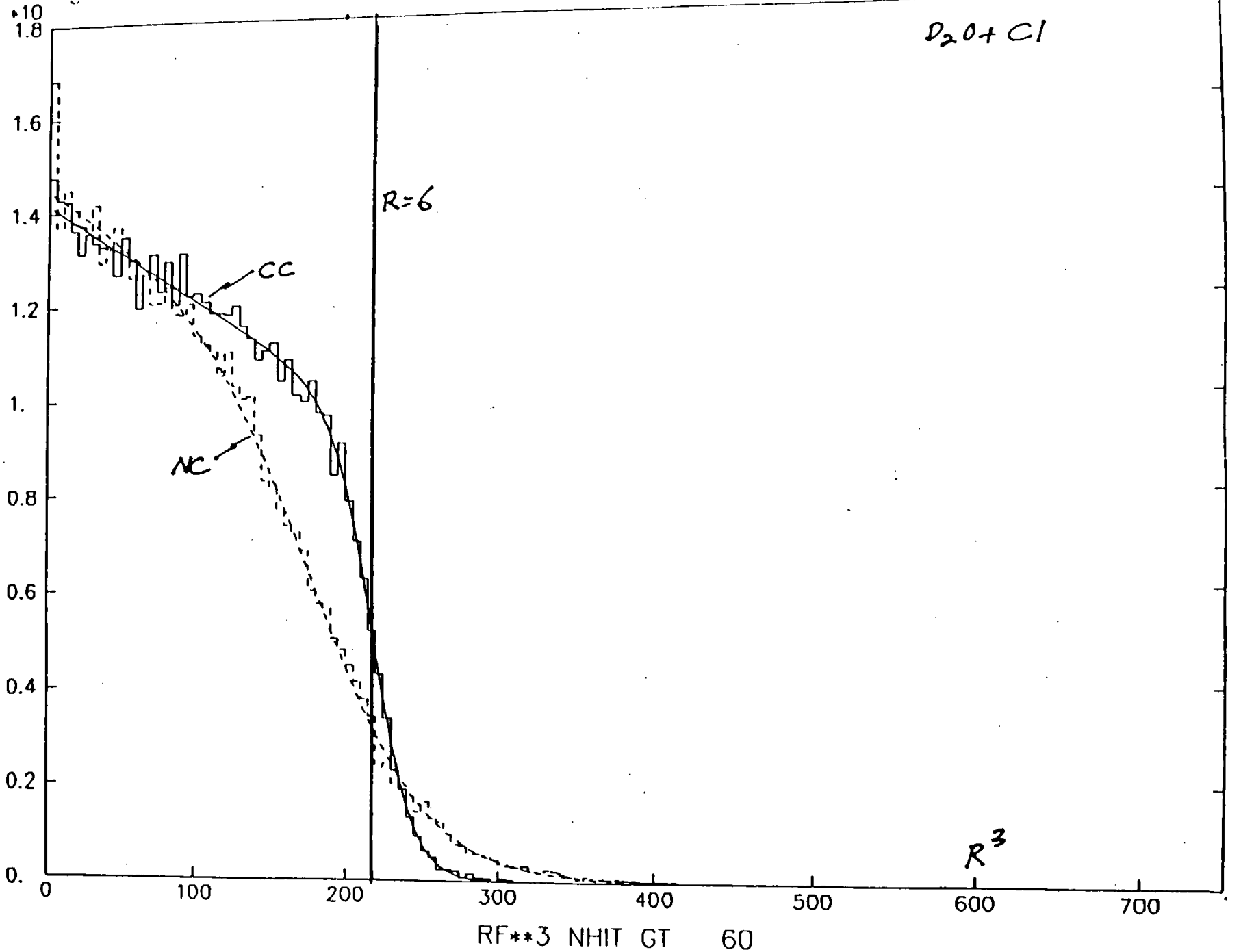
*10
1.8
1.6
1.4
1.2
1.
0.8
0.6
0.4
0.2
0.
0
100
200
300
400
500
600
700
R=6
CC
NC
D2O+Cl
R3
RF**3 NHIT GT 60

Fig 1a

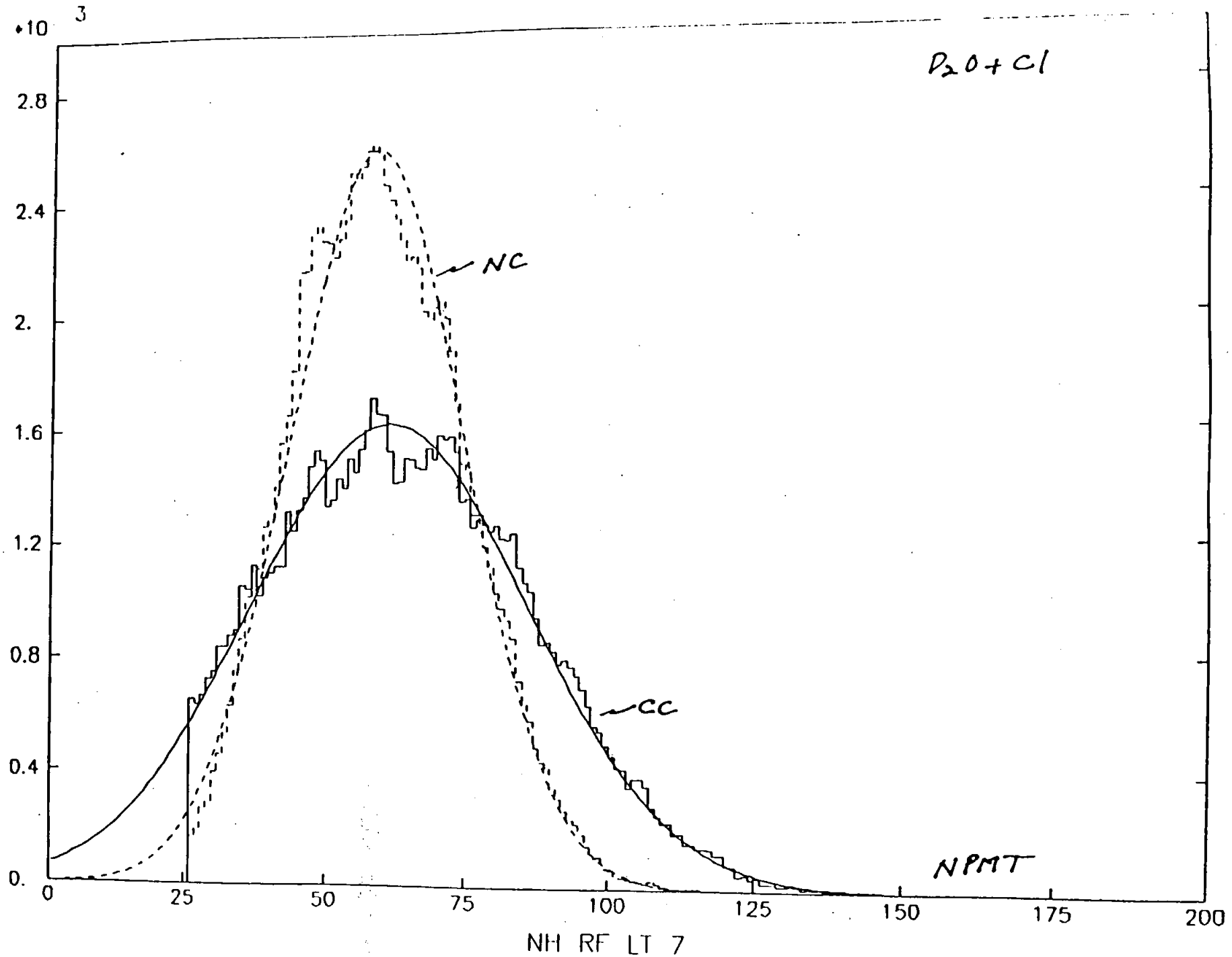
3
•10
2.8
2.4
2.
1.6
1.2
0.8
0.4
0.
0
25
50
75
100
125
150
175
200
NH RF LT 7
D2O + Cl
NC
CC
NPMT

Fig 1b

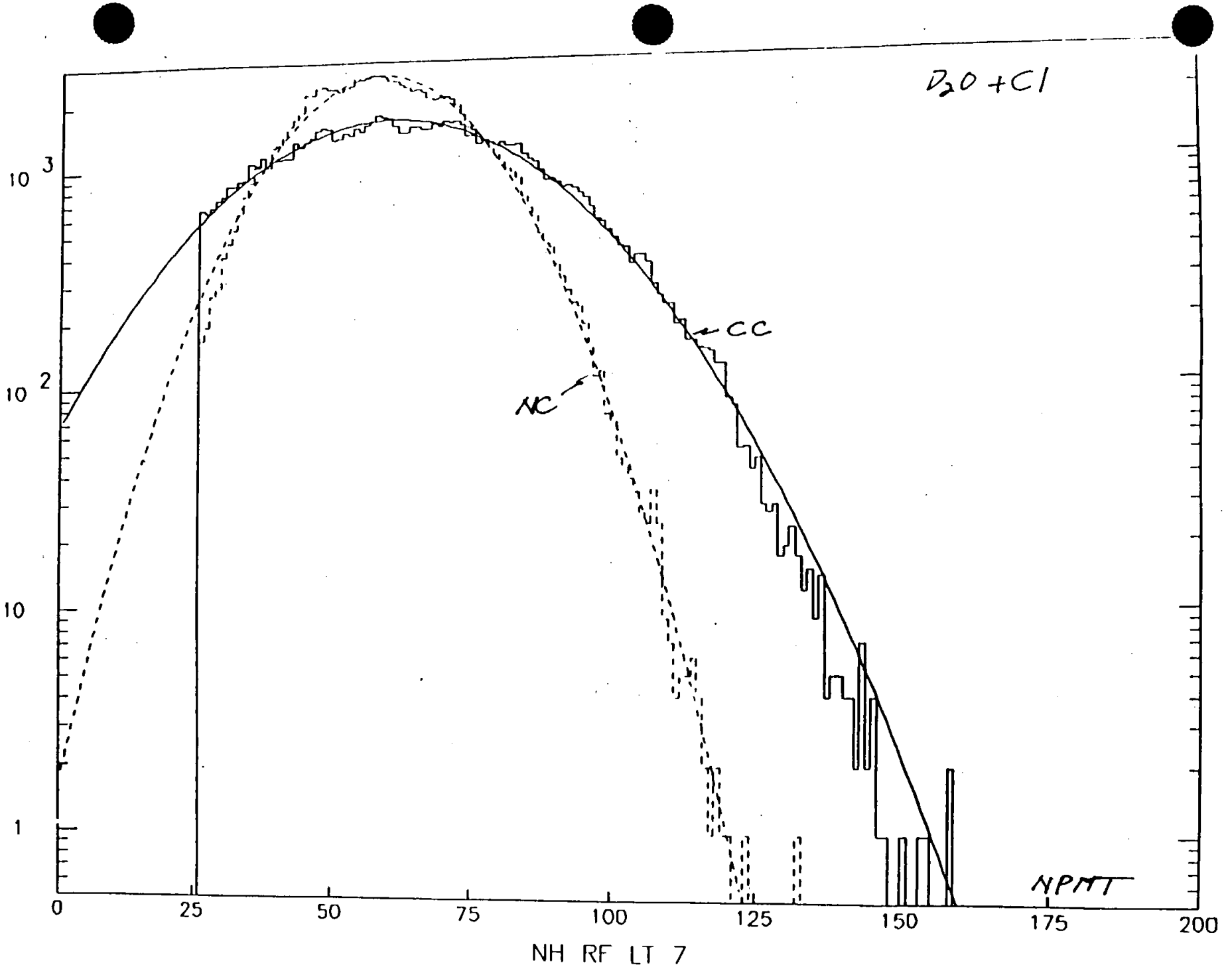
$D_2O + Cl$
CC
NC
NPMT
10^3
10^2
10
1
0
25
50
75
100
125
150
175
200
NH RF LT 7

Fig 1C

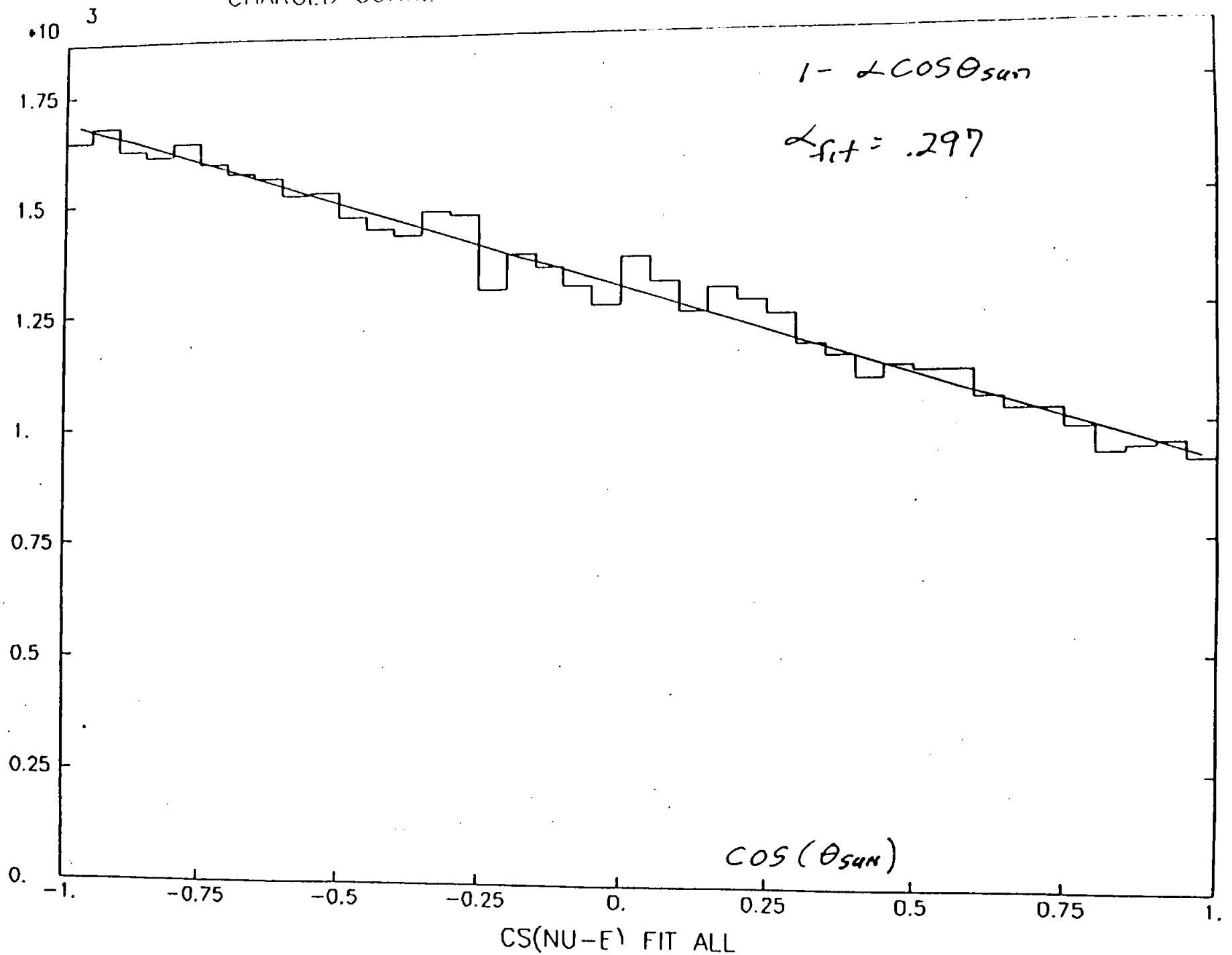
CHARGED CURRENT ANGULAR
3
•10
1.75
1.5
1.25
1.
0.75
0.5
0.25
0.
−1.
−0.75
−0.5
−0.25
0.
0.25
0.5
0.75
1.
$1 - \alpha \cos\theta_{sun}$
$\alpha_{fit} = .297$
$\cos(\theta_{sun})$
CS(NU-E) FIT ALL

Fig 1d

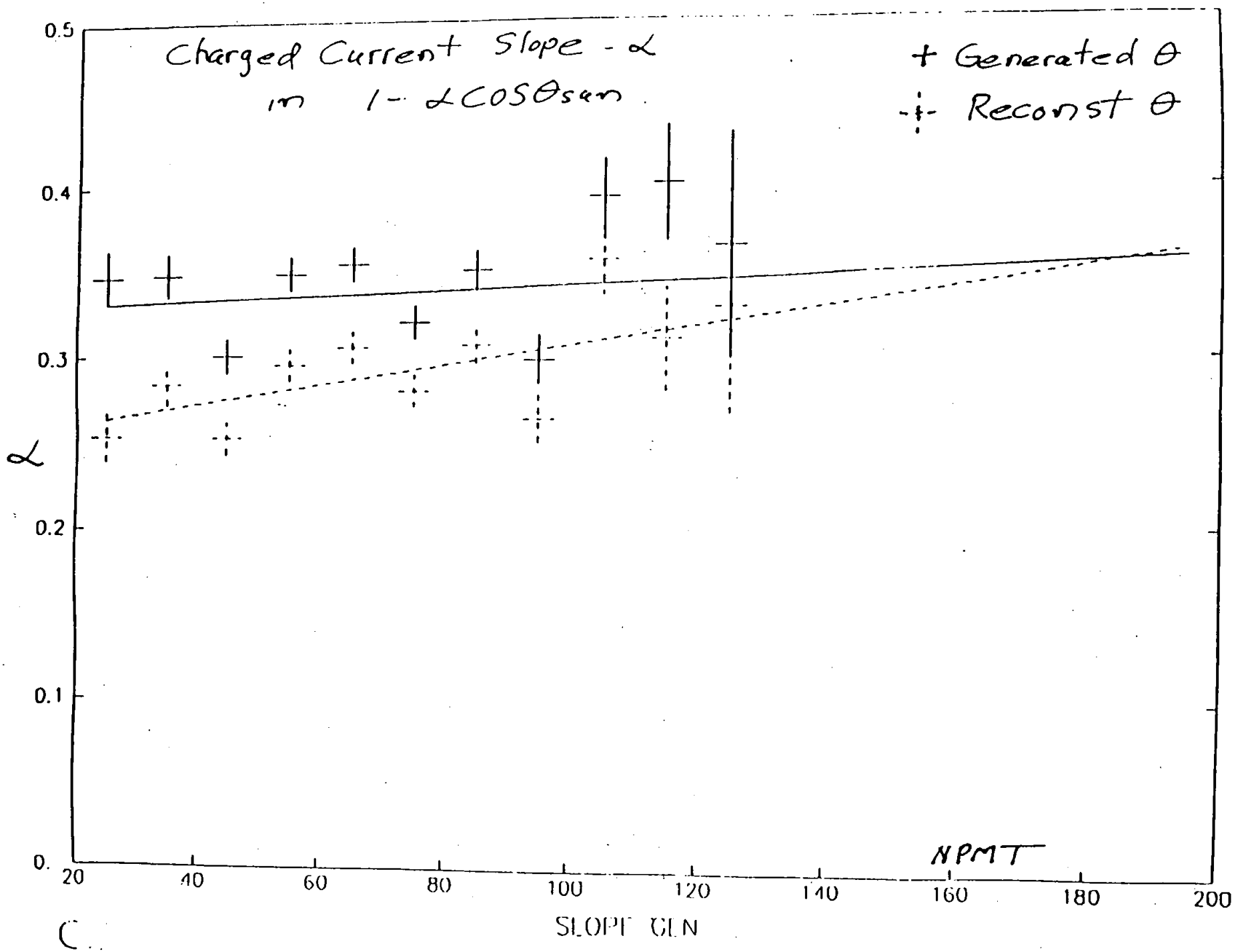
Charged Current Slope - α
in 1 - α COSθsun
+ Generated θ
+ Reconst θ
0.5
0.4
0.3
0.2
0.1
0.
α
20
40
60
80
100
120
140
160
180
200
NPMT
SLOPE GEN

Fig 1C

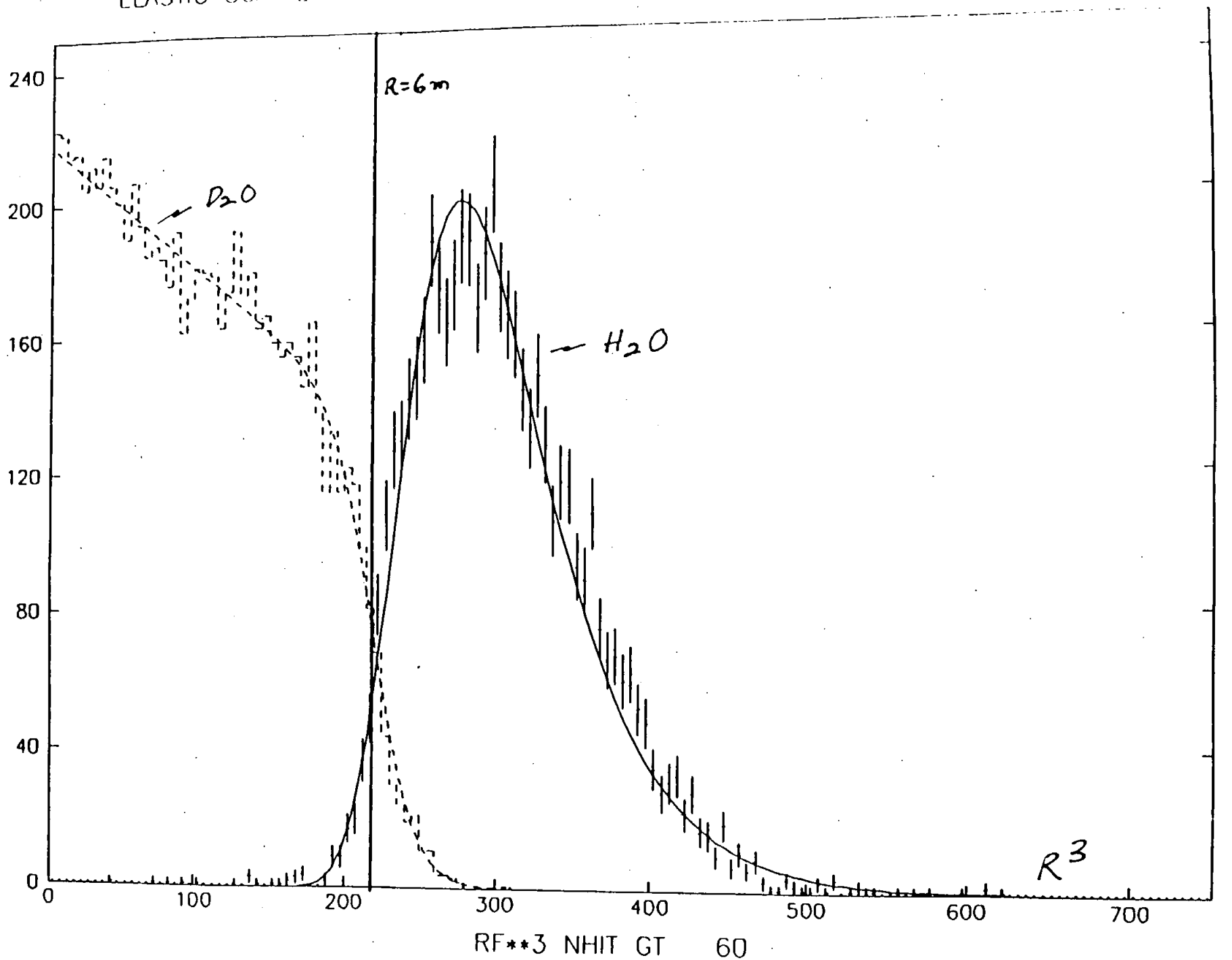
ELASTIC SCATTERING D2O AND H2O
R=6m
D2O
H2O
R3
240
200
160
120
80
40
0
0
100
200
300
400
500
600
700
RF**3 NHIT GT 60

Fig 2a

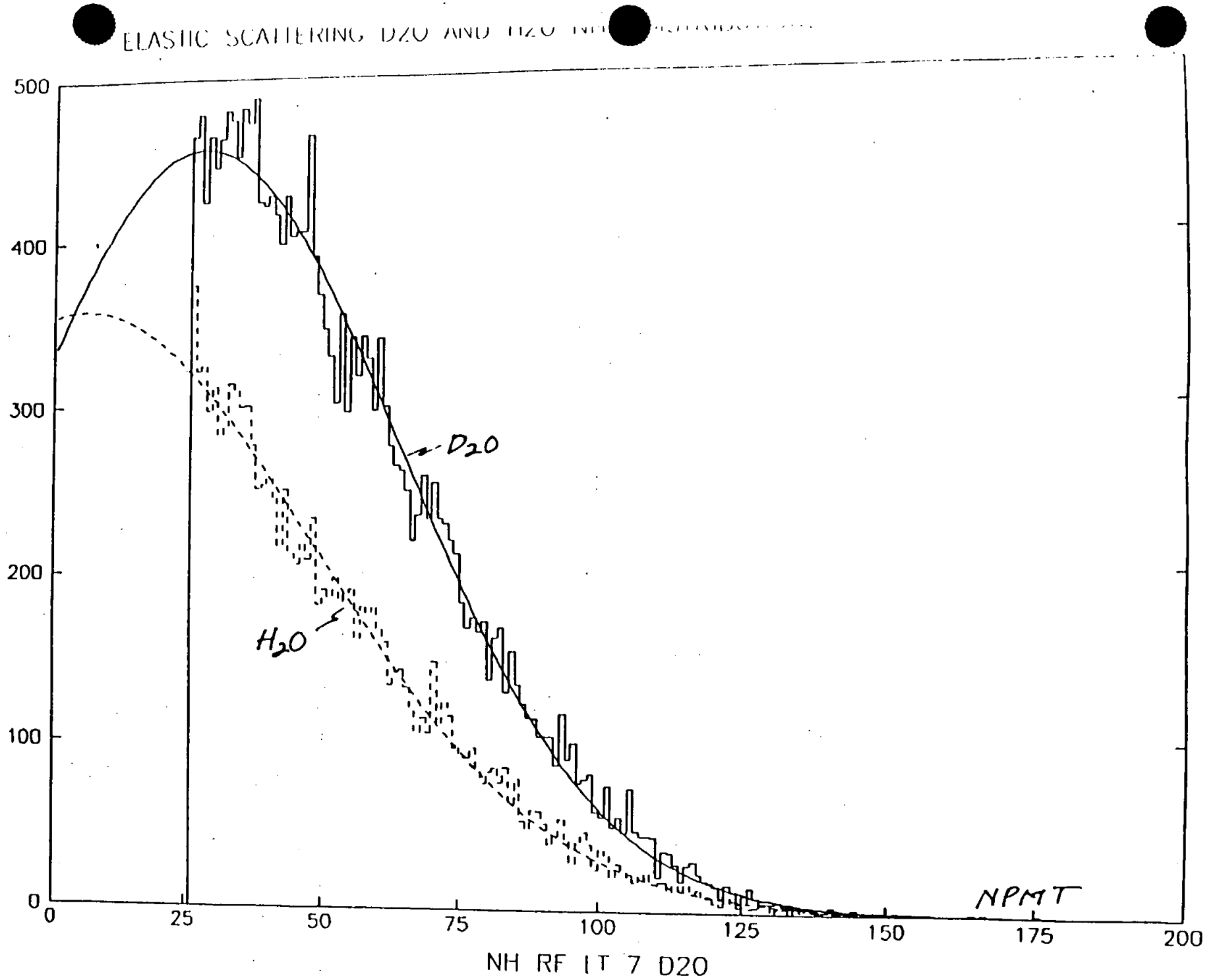
ELASTIC SCATTERING D2O AND H2O
500
400
300
200
100
0
0
25
50
75
100
125
150
175
200
D2O
H2O
NPMT
NH RF IT 7 D2O

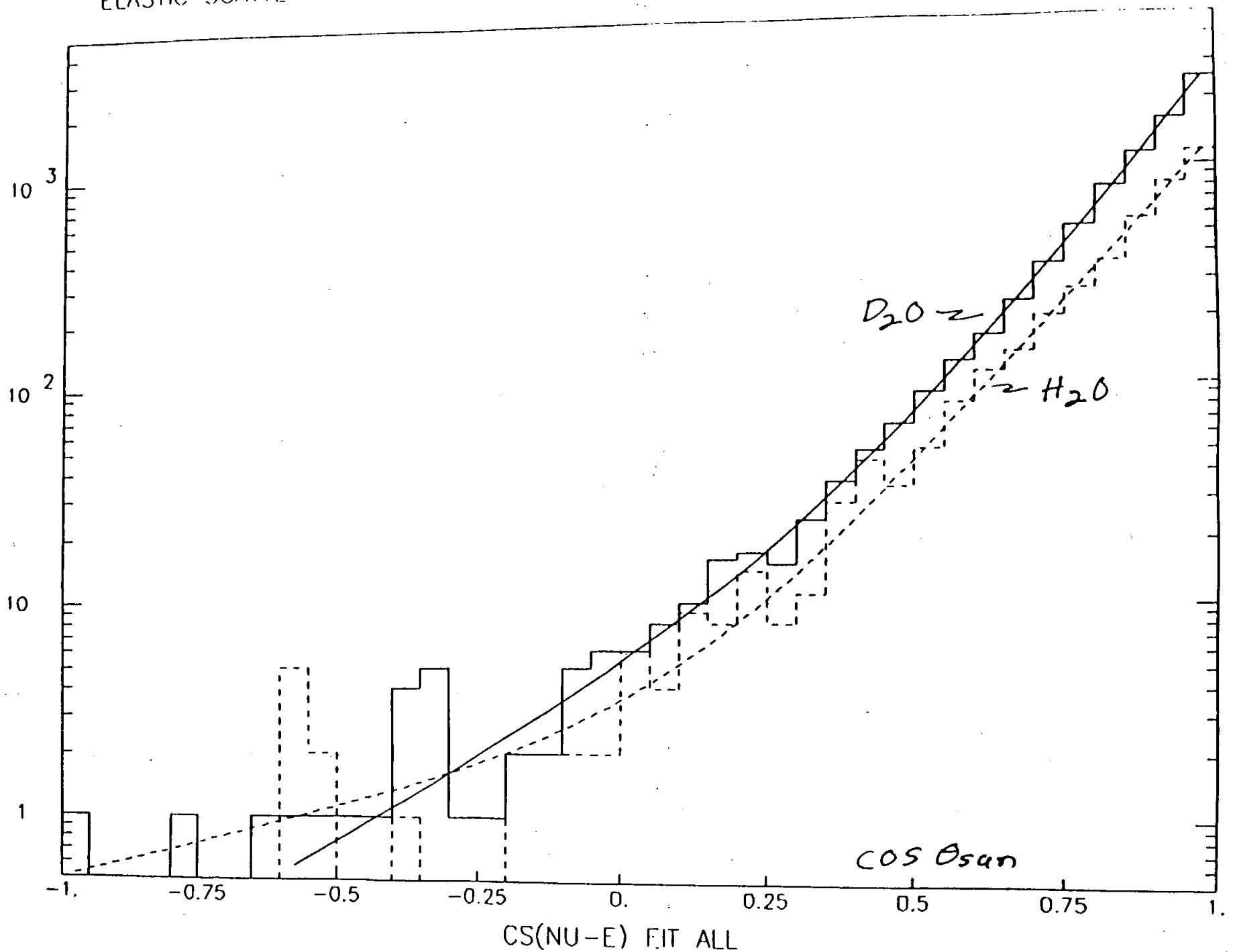
ELASTIC SCATTERING D2O AND H2O COS(
10 3
10 2
10
1
D2O
H2O
COS θsan
-1.
-0.75
-0.5
-0.25
0.
0.25
0.5
0.75
1.
CS(NU-E) FIT ALL

Fig 2C

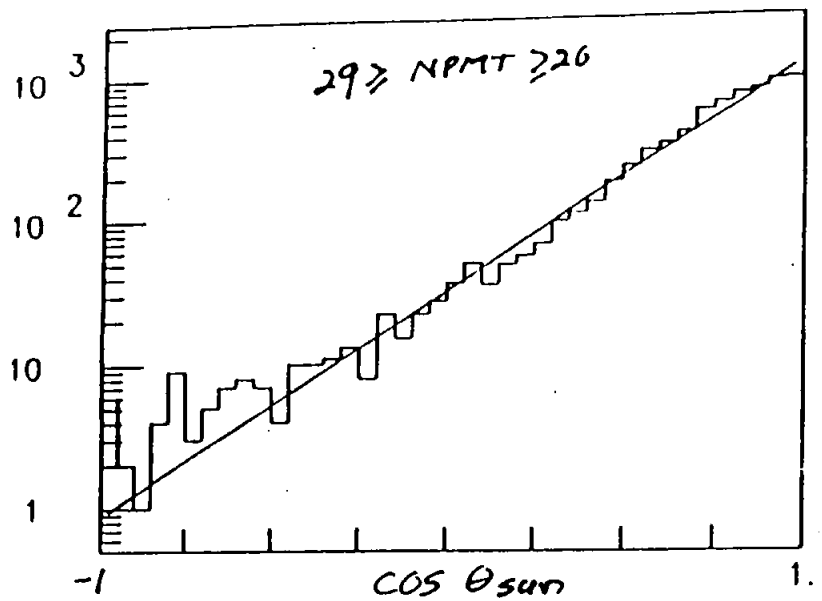

CS(NU-E) 20- 29

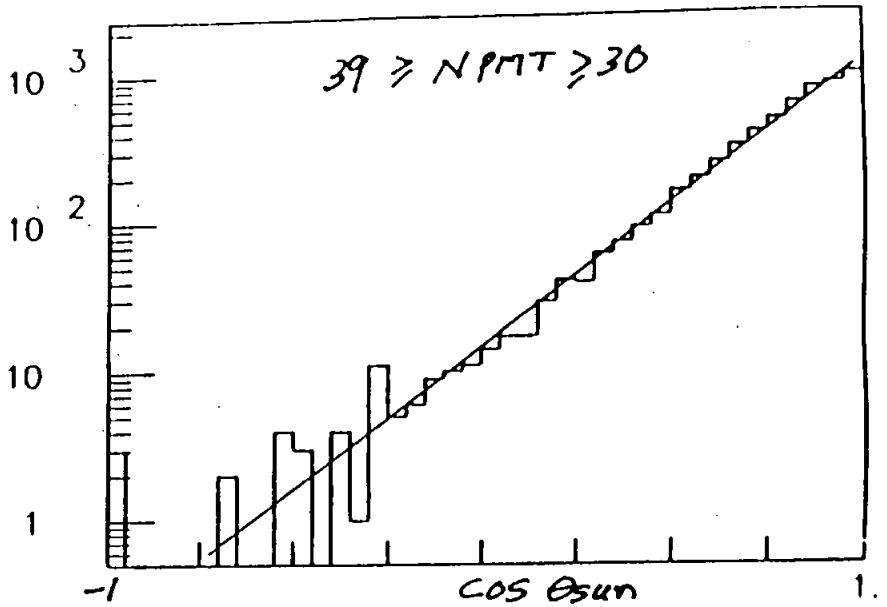

CS(NU-E) 30- 39

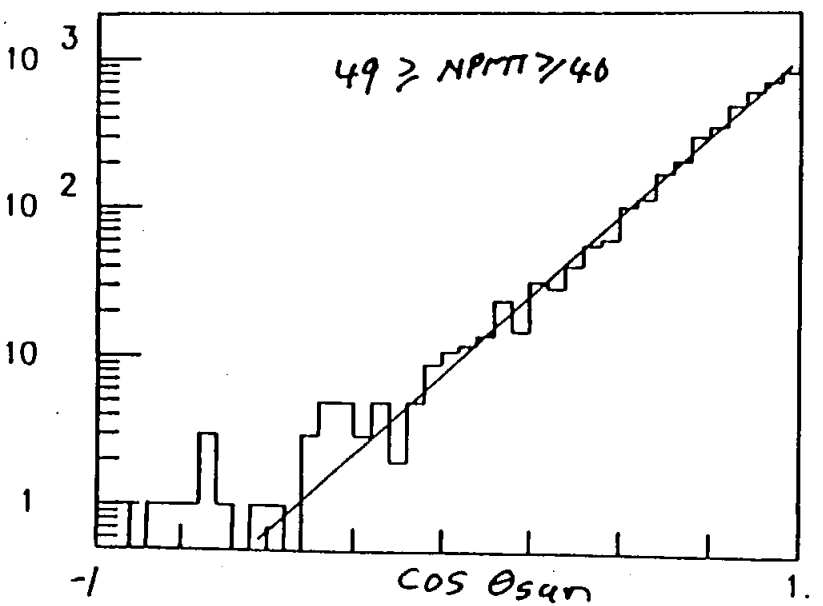

CS(NU-E) 40- 49

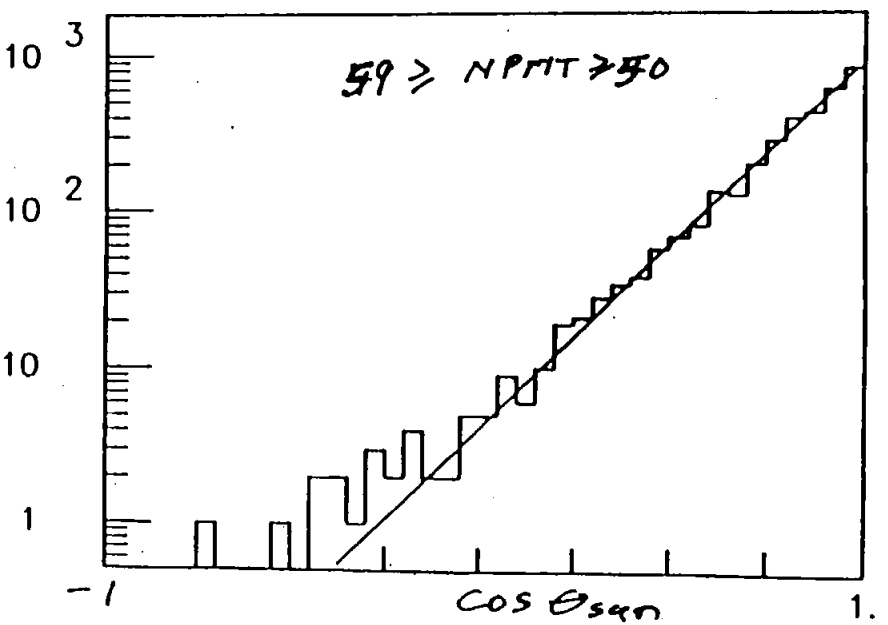

CS(NU-E) 50- 59

Fig 2d

ARESH20A HSTORE

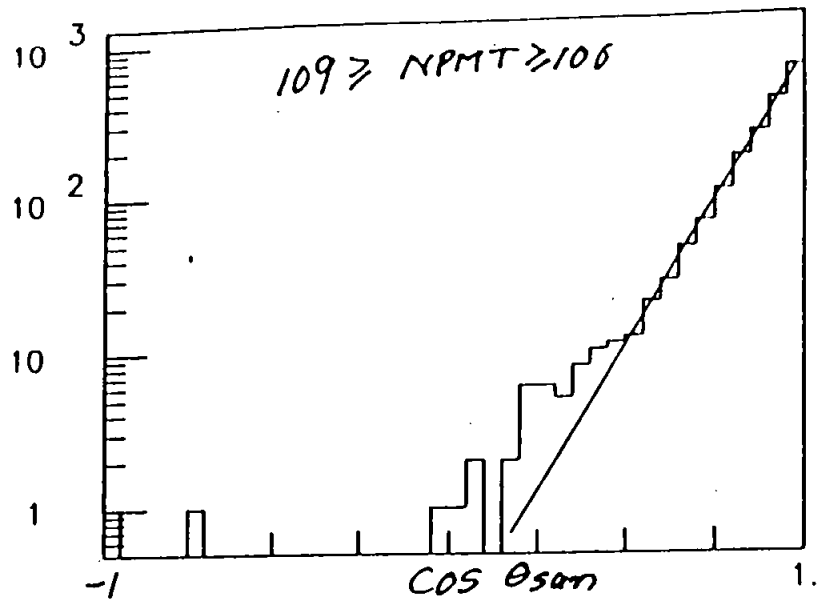

CS(NU-E)100-109

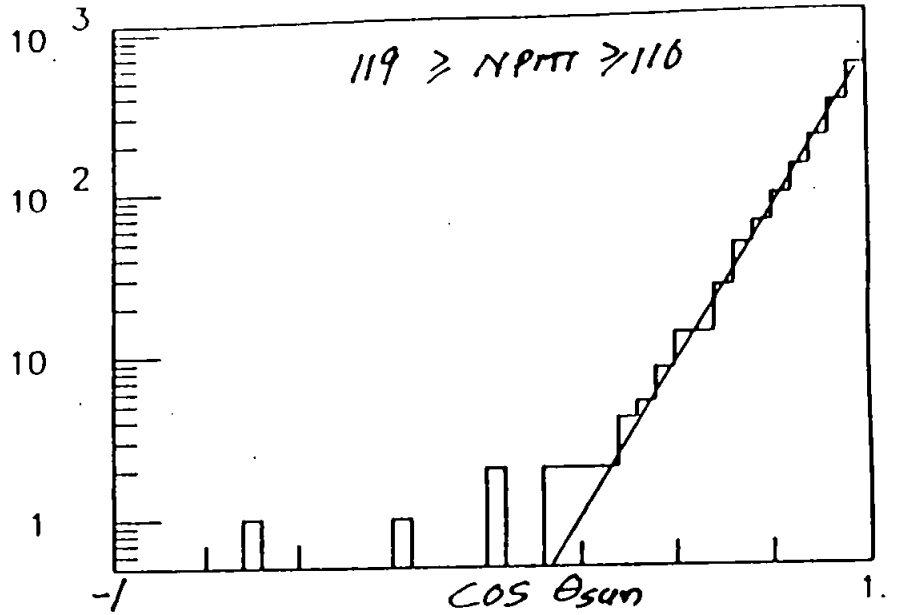

CS(NU-E)110-119

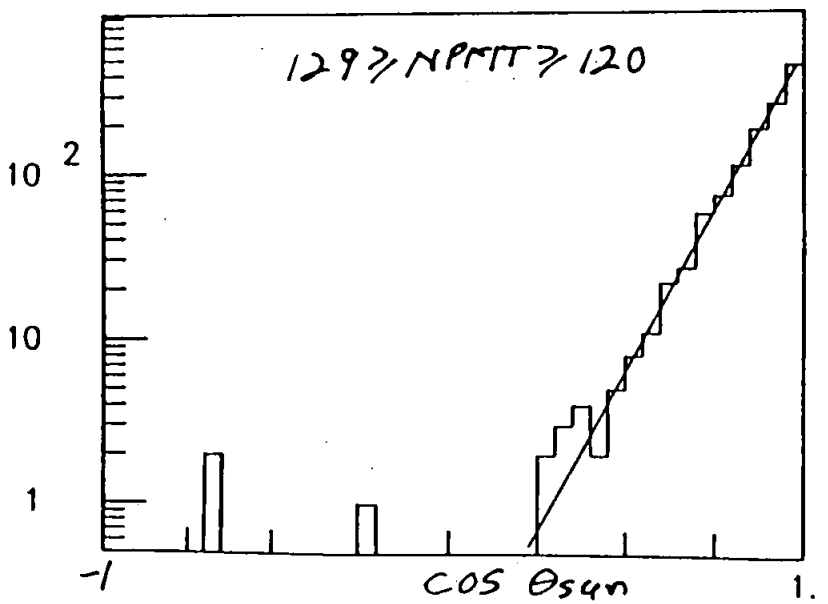

CS(NU-E)120-129

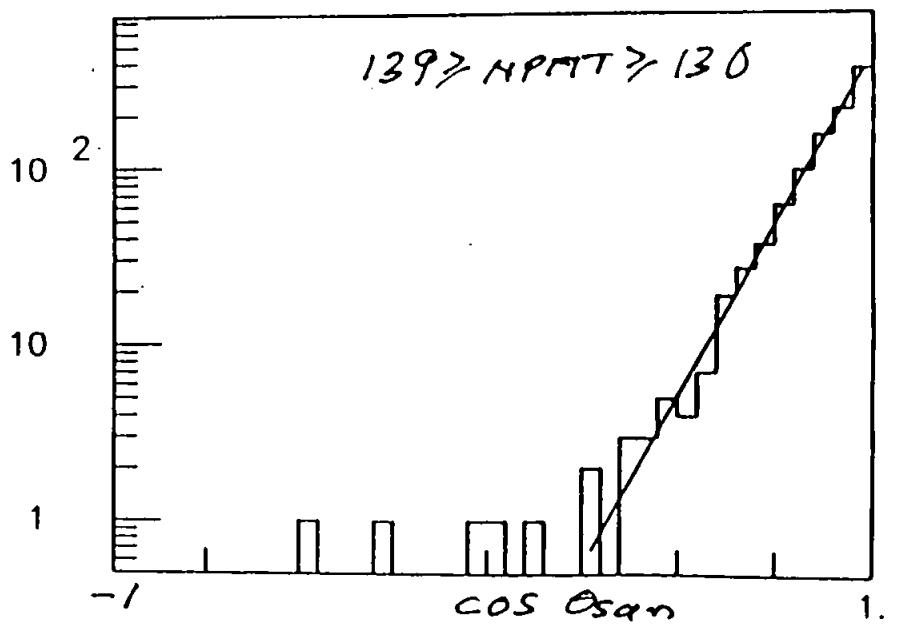

CS(NU-E)130-139

Fig. 3

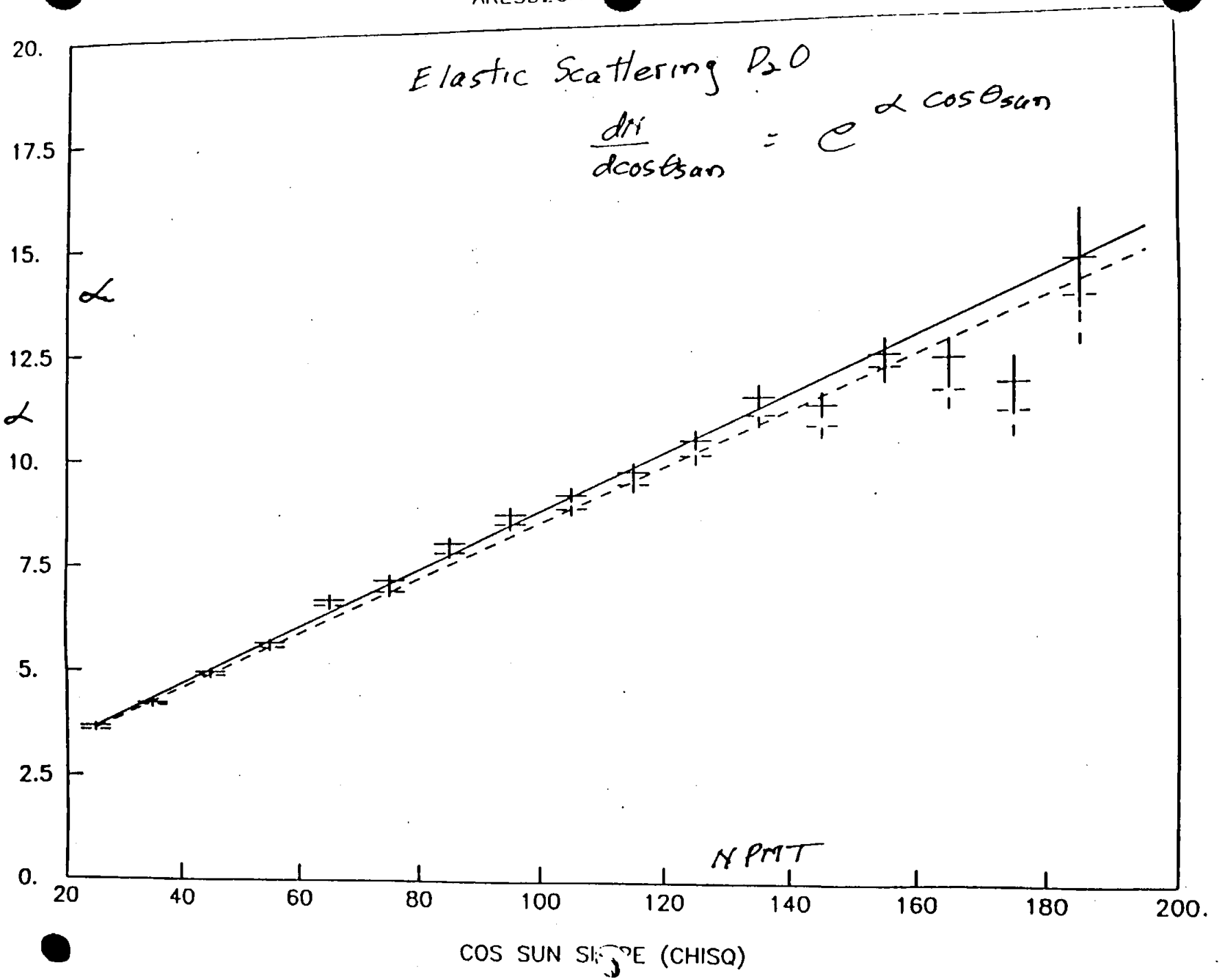
Elastic Scattering D_2O
$\frac{dn}{d\cos\theta_{sun}} = e^{\alpha \cos\theta_{sun}}$
20.
17.5
15.
12.5
10.
7.5
5.
2.5
0.
α
α
20
40
60
80
100
120
140
160
180
200.
N PMT
COS SUN SLOPE (CHISQ)

Fig 2f

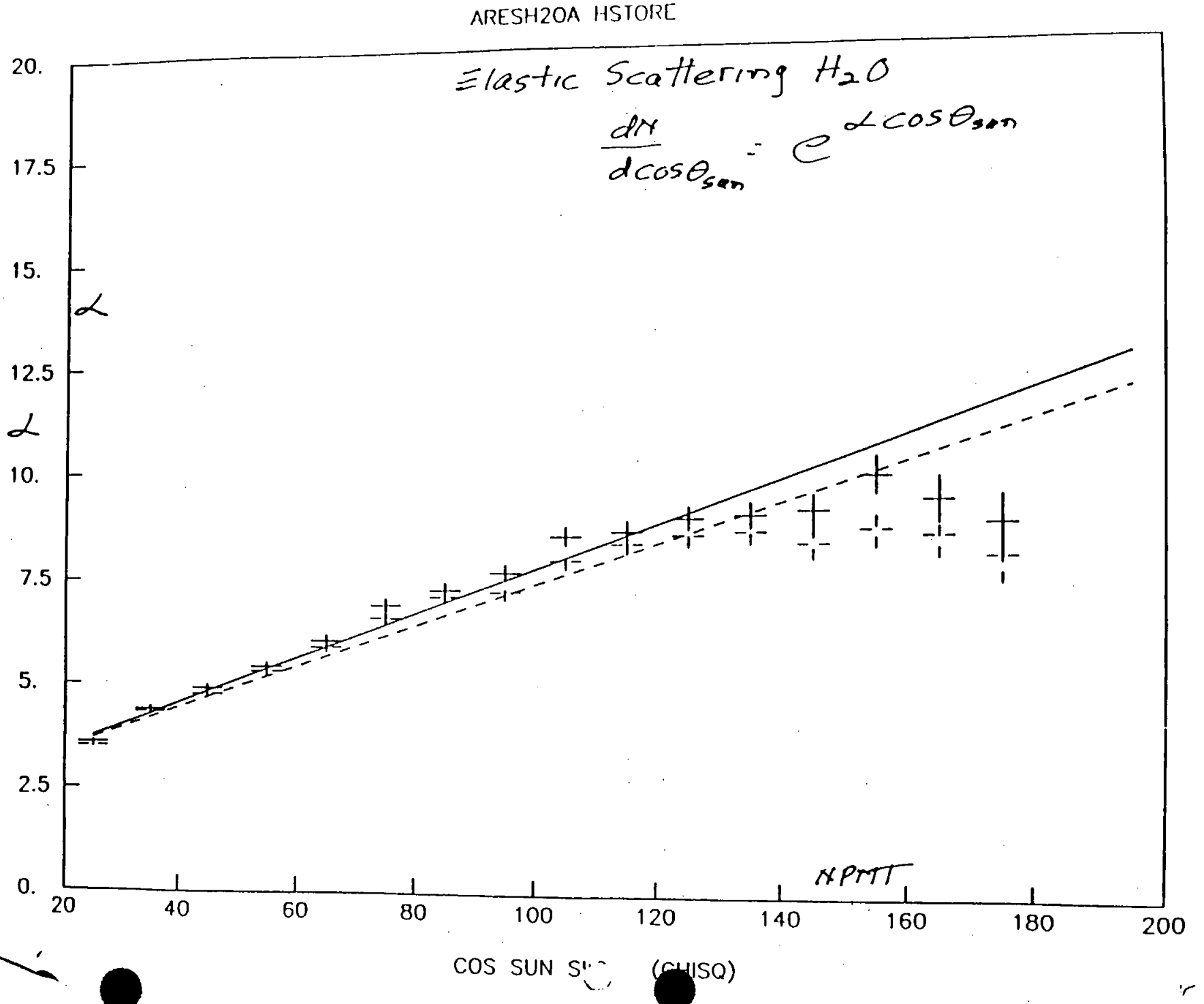
ARESH2OA HSTORE
Elastic Scattering H_2O
$\frac{d\sigma}{d\cos\theta_{sun}} = e^{\alpha \cos\theta_{sun}}$
α
α
20.
17.5
15.
12.5
10.
7.5
5.
2.5
0.
20
40
60
80
100
120
140
160
180
200
NPTT
COS SUN S
(CHISQ)

Fig 29

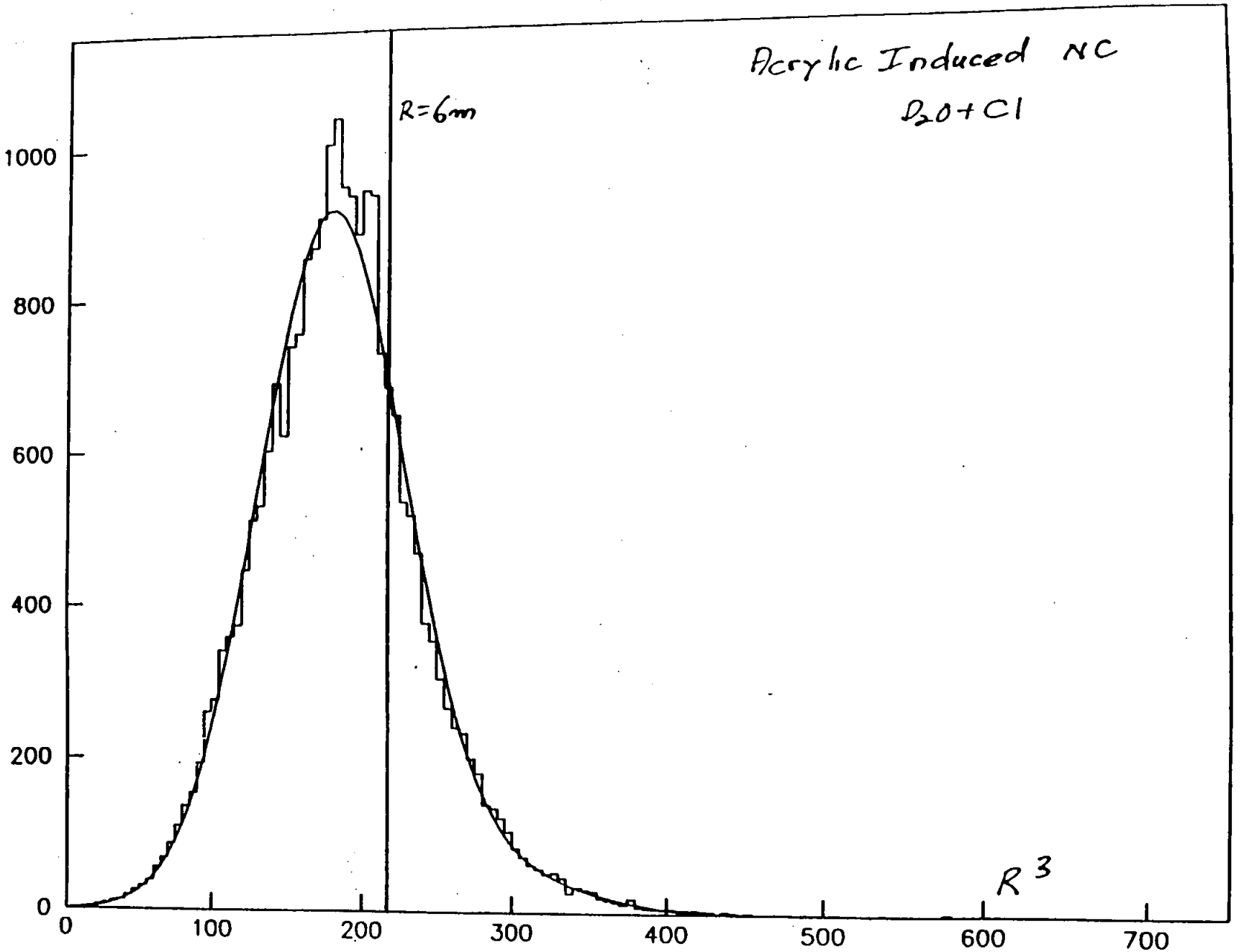

RF**3 NI[illegible] GT 60

Fig 3a